PERIÓDICO TCHÊ QUÍMICA
ARTIGO ORIGINAL

SÍNTESE DOS NANOCOMPOSITOS ESPINÉLIO Mn_3O_4 E ESPINÉLIO Mn_3O_4/ZrO_2 E USANDO-OS NA DECOLORIZAÇÃO FOTO-CATÁLICA DO COMPLEXO Fe(II)-(4,5-DIAZAFLUOREN-9-ONA 11)

SYNTHESIS OF SPINEL Mn_3O_4 AND SPINEL Mn_3O_4/ZrO_2 NANOCOMPOSITES AND USING THEM IN PHOTO-CATALYTIC DECOLORIZATION OF Fe(II)-(4,5-DIAZAFLUOREN-9-ONE 11) COMPLEX

تحضير السبنل Mn_3O_4 والمتراكبات النانوية للسبنل $ZrO_2\backslash Mn_3O_4$ واستخدامهم في الازالة اللونية المحفزة ضوئياً لمعقد Fe(II)-(4,5-DIAZAFLUOREN-9-ONE 11)

HAYAWI, Mohammed Kareem[1]; KAREEM, Mohanad Mousa[2], and AHMED, Luma Majeed [3*]

[1,3]Department of Chemistry, College of Science, University of Kerbala, Karbala, Iraq.

[2]Department of Chemistry, College of Science, University of Babylon, Babylon, Iraq.

** Correspondence author*
e-mail: lumamajeed2013@gmail.com

Received 05 January 2020; received in revised form 03 March 2020; accepted 10 March 2020

RESUMO

A estrutura de espinélio Mn_3O_4 e as partículas de nano-compósitos de espinélio Mn_3O_4/ZrO_2 foram sintetizadas com sucesso como fotocatalisadores, empregando o processo de co-precipitação e a técnica ultrassônica, respectivamente. A morfologia dos fotocatalisadores preparados foi distinguida usando a tecnologia de difração de raios-X (DRX) e microscopia de força atômica (AFM) e indicou que os tamanhos médios de cristal e tamanho de partícula para todas as amostras estudadas eram nanometricas. Além disso, as propriedades ópticas dos fotocatalisadores obtidos foram investigadas usando um espectrofotômetro UV-Vis com acessório de refletância difusa Labsphere para medir as distâncias de banda deles. Com base na equação de Tauc, foram determinados os intervalos de banda (Bg) para os fotocatalisadores estudados. Os intervalos de banda são indiretos para todas as amostras e aumentam os valores para os nanocompósitos com o aumento da quantidade de ZrO_2. Portanto, a sequência dos valores de lacunas de banda é: Bg espinélio Mn_3O_4 <Bg Comp.1 <Bg Comp.2 <Bg Comp.3 <Bg ZrO_2, e igual a 2,21 eV <3,15 eV <4,51 eV <4,26 eV <5,29 eV. A pesquisa revelou que as partículas de nanocompósitos de espinélio Mn_3O_4 e espinélio Mn_3O_4/ZrO2 eram partículas quase esféricas e esféricas, respectivamente. Além disso, foi realizada com sucesso a incorporação da partícula espinélio Mn_3O_4 com a partícula ZrO_2, comprovada por análises de DRX e AFM. Este trabalho descobriu que a resposta da reação fotocatalítica pelo emprego do complexo Fe(II)-(4,5-Diazafluoren-9-ona 11) como material modelo sob lâmpada UV-A com o uso dos fotocatalisadores estudados. Os experimentos fotográficos primários para esses fotocatalisadores descobriram que a descoloração do complexo Fe(II)-(4,5-Diazafluoren-9-ona 11) não é ativa sem a adição de H_2O_2, essa atitude se deve à estabilidade muito alta desses complexos por ter uma estrutura octaédrica, que foi comprovada com o uso do método da razão molar. Considerando que, após a adição de H_2O_2 à solução aquosa desse complexo, verificou-se que a atividade com o nanocompósito de espinélio Mn_3O_4/ZrO_2 3 era o ativo duplo do que com o espinélio Mn_3O_4 sozinho e a sequência da eficiência da descoloração por fotoelétricos (E%) está sendo: E% composto 3 < E% composto 2 < E% composto 1 < E% espinélio Mn_3O_4.

Palavras-chave: *Espinélio Mn_3O_4; Nano-composto espinélio Mn_3O_4/ZrO_2; ZrO_2; Síntese verde e complexo Fe(II)-(4,5-Diazafluoren-9-ona 11)*.

ABSTRACT

The spinel structure Mn_3O_4 and the spinel Mn_3O_4/ZrO_2 nano-composites particles were synthesized successfully as photocatalysts by employing the co-precipitation process and ultrasonic technique, respectively. The morphology of the top mention prepared photocatalysts was distinguished using X-ray diffraction (XRD) technology and atomic force microscopy (AFM) and indicated that the mean crystal sizes and particle sizes for all studied samples were nanometric. In addition, the optical properties of the obtained photocatalysts were

DOI: 10.52571/PTQ.v17.n34.2020.713_P34_pgs_689_699.pdf

investigated using a UV-Visible spectrophotometer with Labsphere diffuse reflectance accessory to measure the bandgaps of them. Based on the Tauc equation, the bandgaps (Bg) for the studied photocatalysts were determined. The bandgaps are indirect for all samples, and it is increased in values for the nanocomposites with the increasing the ratio of ZrO_2 . So, the sequence of bandgaps values is: Bg spinel Mn_3O_4 < Bg Comp.1 < Bg Comp.2 < Bg Comp.3 < Bg ZrO_2, and equal to 2.21 eV < 3.15 eV < 4.51 eV < 4.26 eV < 5.29 eV. The research revealed that the spinel Mn_3O_4 and the spinel Mn_3O_4/ZrO_2 nano-composites particles were quasi-spherical and spherical particles respectively. Moreover, the incorporation of spinel Mn_3O_4 particle with ZrO_2 particle was successfully carried out that was proved by XRD and AFM analyses. This work discovered that the photocatalytic reaction response via employing Fe(II)-(4,5-Diazafluoren-9-one 11) complex as model material under UV-A lamp with the use of the studied photocatalysts. The primary photo experiments for these photocatalysts found that the decolorization of Fe(II)-(4,5-Diazafluoren-9-one 11) complex is not active without addition of H_2O_2, that attitude is due to the very high stability of these complex with having an octahedral structure, which was proved with using mole ratio method. Whereas, after the addition of H_2O_2 to the aqueous solution of these complex, the activity with using the spinel Mn_3O_4/ZrO_2 nanocomposite 3 was found to be the double active than that using the spinel Mn_3O_4 alone, and the sequence of phootdecolorization efficiency (E%) is being: E% composite 3 < E% composite 2 < E% composite 1< E% spinel Mn_3O_4

Keywords: *Spinel Mn_3O_4; Spinel Mn_3O_4/ZrO_2 nano-composite; ZrO_2; Green synthesis and Fe(II)-(4,5-Diazafluoren-9-one 11) complex*.

الملخص

حضر تركيب السبنل Mn_3O_4 وجسيمات المتراكبات النانوية للسبنل Mn_3O_4 \ ZrO_2 بنجاح كعوامل مساعدة ضوئية باستخدام طريقة الترسيب المصاحب وتقنية الموجات فوق الصوتية على التوالي. ميزت الخواص المورفولوجية للعوامل الضوئية المحضرة والمشار اليها اعلاه بوساطة تقنية حيود الاشعة السينية (XRD) ومجهر القوة الذرية (AFM) واشارت الى كون معدل الحجوم البلورية وحجوم الجسيمات لجميع العينات المدروسة هي مواد نانوية.بالاضافة الى ايجاد الخواص الضوئية للعوامل المساعدة الضوئية من خلال استخدام تقنية مطيافية الاشعة المرئية وفوق البنفسجية مع الانعكاس الانتشاري لغرض قياس فجوات الحزم لها. بالاعتماد على معادلة تاوس، حددت فجوات الطاقة (Bg) للعوامل المساعدة الضوئية المدروسة. وجد بان فجوات الطاقة من النوع غير المباشر لجميع العينات، اذا تزداد قيمتها للمتراكبات بزيادة نسبة ZrO_2. لذلك يكون تسلسل قيمها كالاتي: Bg spinel Mn_3O_4 < Bg Comp.1 < Bg Comp.2 < Bg Comp.3 < Bg ZrO_2 والتي تساوي الى 2.21eV < 3.15 eV < 4.51eV < 4.26 eV < 5.29 eV . كشف هذا البحث كون السبنل Mn_3O_4 و المتراكبات النانوية للسبنل Mn_3O_4 \ ZrO_2 هي شبه كروية وكروية الشكل على التوالي. بالاضافة الى ذلك، وجد بان عملية التداخل بين جسيمات السبنل Mn_3O_4 وجسيمات ZrO_2 تمت بنجاح وقد اثبتت بوساطة تحاليل XRD و AFM. في هذا العمل اكتشف بان هنالك استجابة خلال التفاعل المحفز ضوئيا باستخدام معقد Fe(II)- (4,5-Diazafluoren-9-one 11) كموديل للدراسة بوجود مصباح UV-A باستخدام العوامل المساعدة الضوئية المدروسة. وجد من خلال التجارب الضوئية الاولية بان الازالة اللونية لمعقدات Fe(II)-(4,5-Diazafluoren-9-one 11) تكون غير فعالة بدون استخدام H_2O_2 مع هذه العوامل المساعدة الضوئية، ويعزا ذلك للاستقرارية العالية للمعقد وتركيبة الثماني والذي اثبت باستخدام طريقة النسب المولية. ولكن بعد اضافة الـ H_2O_2 الى المحلول المائي لهذه المعقدات، وجد بان الفعالية باستخدام المتراكب رقم 3 من السبنل Mn_3O_4 \ZrO_2 كانت ضعف مقارنة بالفعالية لدى استخدام السبنل Mn_3O_4 لوحدة، حيث كان تسلسل النسبة المئوية للازالة اللونية (E%) كالاتي : composite 3< composite 2 < composite 1< spinel Mn_3O_4

الكلمات المفتاحية: السبنل Mn_3O_4 ، و المتراكبات النانوية للسبنل Mn_3O_4 \ ZrO_2 ، والتخليق الاخضر، و معقدات Fe(II)- (4,5-Diazafluoren-9-one 11)

1. INTRODUCTION

The Mn_3O_4 (Hausmannite) is a standard spinel compound, indicating the distribution of Mn(II) in tetrahedral and Mn(III) in octahedral locations, this coupling compound can also be written as $Mn^{2+}O.Mn_2^{3+}O_3$ ($MnO.Mn_2O_3$) formula (Goodenqugh and Loeb, 1955; Fritsch *et al*., 1998). Despite the Mn(II) and Mn(III), there are large magnetic moments, but Mn_3O_4 is considered a paramagnetic as low as 72 K, but it is ferromagnetic at below 43 K and connected by covalent forces to create a spinel structure with semi-covalent exchange (Goodenqugh and Loeb, 1955; Boucher *et al*., 1971a; Boucher *et al*., 1971b). The structure of spinel Mn_3O_4 is arranged in the unit cell as 24 cations with 32 oxygen atoms (Fritsch *et al*., 1998; Pike *et al*., 2007). The common crystal structure of the spinel Mn_3O_4 is tetragonal with lattice parameters (*a* equal to *b)* = 5.762 Å but *c* = 9.4696 Å (Pike *et al*., 2007). At 1170 °C, Mc Murdie (McMurdie *et al*., 1950). found that the tetragonal crystal structure can be translated into a cubic crystal structure.

There are varies routes to prepare the spinel Mn_3O_4 as bulk and nanoparticles catalysts such as soft template self-assembly (Zhang *et al*., 2010), a hydrothermal method (Yao *et al*., 2018; Shah *et al*., 2016), gas-liquid reaction method (Cui *et al*., 2014), precipitation method (Vijayalakshmi *et al*., 2014), chemical bath deposition method (Zhao *et al*., 2015) and using the microwave irradiation technique (Bousquet-

Berthelin *et al*., 2015). The spinel Mn_3O_4 is considered to be one of the most stable oxides of manganese, thus raising the interest in its use as electrode materials (Themsirimongko *et al*., 2016; Bikkarolla *et al*., 2014), as poisonous metal adsorption (Silva *et al*., 2012) and as a catalyst in multiple oxidation and reduction reactions (Li *et al*., 2013). The spinel Mn_3O_4 surface is modified by integrating it with other metal oxides as a composite to enhance the effectiveness of the reactions such as NiO (Rahaman *et al*., 2000), CdO (Deepa *et al*., 2013), Fe_2O_3 (Mohammad *et al*., 2014), Al_2O_3 (Asif *et al*., 2015) and ZnO (Senthilkumar *et al*., 2015).

The purposes of this work are; to prepare the spinel Mn_3O_4 by the precipitation method, to prepare its composite with ZrO_2 by the ultrasonic method as a green technique, to measure the morphology and optical properties of both, and to exam them on photodecolorization of a colored solution prepared from Fe(II)-(4,5-Diazafluoren-9-one 11) complex, which is high stable.

2. MATERIALS AND METHODS

All the chemicals were used as received without further purification, Manganese (II) acetate tetrahydrate $Mn(CH_3COO)_2{\cdot}4H_2O$, Sodium carbonate ($Na_2CO_3$) were purchased from BDH Company, England. 1,10-Phenanthroline, Potassium oxalate ($K_2C_2O_4.H_2O$), and Zirconium(IV) oxide were supplied from Riedel-De-Haen AG, Seelze, Hannover, Germany. Iron (II)sulfate heptahydrate ($FeSO_4.7H_2O$), Iron (III)sulfate hydrate ($Fe_2(SO_4)_3.H_2O$), Hydrogen peroxide (H_2O_2), Absolute ethanol (C_2H_5OH), Hydrochloric acid (HCl) and Sodium hydroxide (NaOH) were of analytical grade and obtained from various sources. Fe(II)-(4,5-Diazafluoren-9-one 11) complex were prepared in the physical-chemistry laboratory at the University of Kerbala, college of science, department of chemistry, as shown in Equation 1.

The metal: ligand ratio is 1:3, and it has high stability constant equal to 7.575×10^4, this value was calculated from data of mole ratio (Hadjiioannoy *et al*., 1988; Ingle *et al*., 1988) at wavelength 510 nm or FeL_3, as represented in Figure 1 and Equations 2 to 4.

2.1. Instrumentation

The main instruments that were applied in the study of the characterization of the prepared nanomaterials were an X-Ray Diffraction Spectroscope, model Lab X- XRD 6000, Shimadzu, Japan. A UV-Visible spectrophotometer, model AA-1800, Shimadzu Japan. An AFM, model AA 3000, Advanced Angstrom Inc., USA. A UV-Visible spectrophotometer with Labsphere diffuse reflectance accessory (Varian Cary 100 Scan, Laposphere- 99-010, Maryland United States). Furthermore, a furnace (type Muffle furnace Size-Tow Gallenkamp, England), a pH meter (type OAICTON-2100, Singapore), a ultrasonic bath (DAIHAN Scientific, Korea), a centrifuge (Hettich-Universal II- Germany), a magnetic stirrer (Heido-MrHei-Standard, Germany), and a sensitive balance (BL 210 S, Sartorius, Germany) were employed as essential and simple instruments in this procedure.

2.2. Synthesis of the Spinel (Mn_3O_4) as photocatalyst

A 1 M solution of sodium carbonate (precipitating agent) was added as drop by drop in the solution of $Mn(CH_3COO)_2.4H_2O$ under vigorous mixing, and constant heating from 70°C to 75 °C. From this mixture, the Manganese was precipitated as $MnCO_3$ under controlled pH (9.0). The produced suspension was stirred for 2 hours at the constant temperature to complete the digestion process. After that, a pale pink precipitate of $MnCO_3$ was filtered using Wattmanilter paper no. 1, washed with hot reagent water type IV, and then it was dried at 120 °C for 24 hours. After that, the obtained powder of $MnCO_3$ was well crushed by using a mortar and later oxidized under burn at 600 °C with a suitable quantity of oxygen, which leads to producing a dark brown powder from the spinel Mn_3O_4. The growth of the spinel Mn_3O_4 was elucidated on the happening of the hydrolysis stage of $Mn(CH_3COO)_2.4H_2O$ and then the oxidation stage of the produced $MnCO_3$ by the chemical reactions described by Equations 5 and 6 (Palache *et al*., 1944).

2.3. Synthesis of the (Spinel Mn_3O_4/ ZrO_2) nanocomposites as photocatalysts

After the preparation of the spinel Mn_3O_4, the spinel Mn_3O_4/ZrO_2 nanocomposites were directly prepared by using an ultrasonic technique, which provides the reaction with the necessary energy to combine them. The prepared spinel Mn_3O_4 and commercial ZrO_2 were employed as starting precursors for preparing these nano-composites in ratios of Mn_3O_4:ZrO_2 equal to (1:2), (1:3) and (1:4) respectively. The mention ratios of the nanocomposites were prepared directly by using ultrasonic as a green technique that has appropriate energy to generate the bond between Mn and Zr in a crystal lattice.

Exactly 2.5 g, or 1.66 g , or 1.25 g of Mn_3O_4 was dispersed in distilled water using an ultrasonic bath at a frequency equal to 60 kHz for 4 h. On the other hand, (5.0) g of ZrO_2 was also dispersed in distilled water at the same conditions, which deemed as enough energy for bonding Mn with Zr in a crystal lattice. These solutions were combined, and then ultrasonically irradiated for 1 h. The produced suspension was stirred at 70 °C for 30 min, and it produced a dark gray precipitate. The final precipitate was washed with hot distilled water (reagent water type IV) several times, filtered and dried at 100 °C.

The structural characteristics of all studied samples were examined at an X-ray diffractometer with Cu kα radiation (λ= 0.15406 nm). The morphology of photocatalyst and photocomposite was performed by atomic force microscopy. The bandgaps for all samples were calculated from the data of using UV-Visible spectrophotometer with Labsphere diffuse reflectance accessory.

2.4. Application of the spinel Mn_3O_4 and the spinel Mn_3O_4/ZrO_2 nanocomposites on the decolorization of colored solution.

This application was implemented using a homemade photoreactor, which consisted of a Philips UV-A lamp (400 watts) with a light intensity equal to 3.189×10^{-7} Einstein.s^{-1}, wooden box, magnetic stirrer, Teflon bar, 500 mL Pyrex glass beaker, and fan.As represented in scheme 1. The 0.1 g of the spinel Mn_3O_4 and Spinel Mn_3O_4/ZrO_2 nanocomposites were added to 50 mL from a solution of Fe(II)-(4,5-Diazafluoren-9-one 11) complex with 0.5% to 30% of H_2O_2. This photoreaction was first performed in the dark as a physical adsorption process, for 15 min at 15 °C, to contact the active sites of the prepared photocatalyst with the complex and the H_2O_2.

Samples of approximately 2.5 mL of the mixture were collected every 5 min of irradiation and separated two times by centrifuge. The clear solution was analyzed using a UV-visible spectrophotometer at 510 nm. The rate constant of this photoreaction (Hussein *et al*., 2018; Ahmed *et al*., 2018 a) and the efficiency of decolorization (Ahmed *et al*., 2018 b; Kzar *et al*., 2019; Rangel *et al*., 2018) were calculated using Equations 7 and 8.

$$ln\left(\frac{A_o}{A_t}\right) = k_{app.}t \qquad \text{(Eq. 7)}$$

$$E_{decol.}\% = \left(\frac{A_o - A_t}{A_o}\right) x\ 100 \qquad \text{(Eq. 8)}$$

In Euqations 7 and 8, A_o is the initial concentration of complex without illumination (dark reaction for 15 min), and A_t is the concentration of the complex at time *t* (in min) of illumination.

3. RESULTS AND DISCUSSION:

In order to investigate the crystalline phases of the synthesized catalyst samples, the X-Ray powder diffraction analysis was performed, results in Figure 2. All the strong and sharp diffraction peaks were successfully refined with the tetragonal phase of Mn_3O_4 (Vijayalakshmi *et al*., 2014; Zhao *et al*., 2015) that is compatible with the reference JCPDS 24-0734, which is referred no new peaks of impurities were observed (Zhao *et al*., 2015; Li *et al*., 2013). The mean crystallite size (L) of the prepared spinel Mn_3O_4 nanoparticle was detected from the significant (211), (103) and (224) diffraction peaks with the employing the Debye-Scherrer Equation (9) (Rangel *et al*., 2018; Mohammed and Ahmed., 2018; Fakhri and Ahmed, 2019).

$$L = \frac{k\,\lambda}{\beta\ Cos\ \theta} \qquad \text{(Eq. 9)}$$

Where, λ is the wavelength of Cu as the source of the instrument in (nm), k is shaped constant , β is the full width at half maximum intensity in (radian), and θ is the Bragg diffraction angle.

The mean crystallite size of the prepared spinel Mn_3O_4 nanoparticle was calculated to be equal to 32.775 nm.

The XRD peaks in Figure 3 proved that the nanocomposites of the prepared spinel Mn_3O_4 nanoparticle with commercial ZrO_2 in ratios (1:2), (1:3) and (1:4) respectively, were actually created between Mn bond and Zr bond in crystal lattices. The mean crystallite sizes for all mention prepared photocatalysts are estimated as 25.411 nm, 25.7504 nm, and 12.994 nm, respectively. Moreover, new peaks at 2θ equal to 23.80° -23.90°, 28.12° -28.18°, 31.34°-31.40°, 39.96°- 40.26°, 49.50°-50.04° are noted at miller indexes (110), (011), (111), (020), (012), (022) corresponding to the m-ZrO_2 phases (Vaizoğullar *et al*., 2016) (JCPDS 37-1484). For the Mn_3O_4, the peak for 44.3° at (220) is shifted to a high 2θ value when nanocomposites are created, that attitude to incorporate two metals (Mn with Zr)

into the new bond. This behavior is consistent with the study in references (Mahammed and Ahmed, 2017; Ahmed *et al*., 2014).

3.1. Surface Morphology of photocatalyst

The Atomic force microscopy (AFM) images were displayed in Figure 4, it is noted that the particle size of Mn_3O_4 is 58.33 nm. It is smaller than that values for Mn_2O_3/ZrO_2 nanocomposites 1, 2, and 3, which equals 93.71 nm, 88.24 nm, and 73.14 nm, respectively. This is attributed to the low ionic radius of the Mn^{2+} (0.66 Å) and Mn^{3+} (0.64 Å) compared with the ionic radius of Zr^{4+} (0.747 Å) (Ghosh and Biswas, 2003). Moreover, Mn_3O_4/ZrO_2 nanocomposites have more agglomeration than the Mn_3O_4 sample.

3.2. Optical Absorption Study

Based on the extrapolation of the peaks of samples employing the Tauc equation plots (Fakhri and Ahmed, 2019; Brijnandan *et al*., 2017; Augustine and Nnabuchi, 2017) in Figure 5, the indirect bandgaps for spinel Mn_3O_4, and its nanocomposites 1, 2 and 3 with ZrO_2 were detected and discovered to rise from approximately 2.1 eV for Mn_3O_4 to 3.75 eV, 4.51 eV and 4.65 eV for nanocomposites 1, 2 and 3 respectively. The increase of bandgaps is indicated to decreased the mean crystal size of nanoparticles, so composite 3 is having the maximum bandgap 4.65 eV with less mean crystal size (12.994 nm) and particle size (73.14 nm).

3.4. Photocatalytic decolorization of Fe(II)- (4,5-Diazafluoren-9-one 11) complex

In order to evaluate the photocatalytic activity of the prepared spinel Mn_3O_4 nanoparticles and its nanocomposites 1, 2, and 3, the decolorization of Fe(II)-(4,5-Diazafluoren-9-one 11) complex was performed without and with presence H_2O_2 (strong oxidant agent), according to Equations 10-12.

The addition of H_2O_2 will produce further hydroxide radical (Ahmed *et al*., 2018 c) under UV-A light.

$$H_2O_2 + hv \rightarrow 2HO^{\cdot} \qquad \text{(Eq.12)}$$

Figure 6 illustrates that the rate of reaction and the decolorization efficiency of Fe(II)-(4,5-Diazafluoren-9-one 11) complex increase with addition H_2O_2 and using the incorporated of Mn_3O_4 with ZrO_2 as nano-composite 1, nano-composite 2 and nano-composite 3. That due to raising the acidity of the Mn_3O_4 surface via incorporated it with ZrO_2 crystal lattice. That increases the amount of produced hydroxyl radical at pH 4 (natural pH of Fe(II) solution) in the presence of hydrogen peroxide, as shown in Equations 10 and 11 (Abbas *et al*., 2019; Ahmed *et al*. 2012). The efficiency of the photodecolorization of this complex with the use of nano-composite 3 is twice the amount than the use of prepared Mn_3O_4 and reached 40% in 1 h that due to have it a low mean crystal size and particle size compared with other synthesis nano-composite (Fakhri and Ahmed, 2019).

4. CONCLUSIONS:

On the depended of the occurred results, the following conclusions may be written:

1- The prepared spinel Mn_3O_4 and the spinel Mn_3O_4/ZrO_2 nanocomposites have been synthesized by the precipitation method and the direct ultrasonic method, respectively.
2- The XRD data conclude that the spinel Mn_3O_4 is actually prepared by precipitation method and should be tetragonal with an indirect bandgap equal to 2.1 eV.
3- All the prepared samples are polycrystalline and contain from 3 to 6 crystals.
4- The mean crystal size and particle size for spinel Mn_3O_4 are lower than for prepared nanocomposites 1, 2, and 3 readies with significant indirect band gaps of 3.15 eV, 4.51 eV, and 4.62 eV respectively.
5- The nanocomposite 3 is more active in the photodecolorization of Fe(II)-(4,5-diazafluoren-9-one 11) complex in the presence of H_2O_2 compared with other samples, and the photoreaction for this obeys to first-order kinetics.

5. ACKNOWLEDGMENTS:

The authors are grateful to all the persons who assisted in this project during performed it at the University of Kerbala, college of science, department of chemistry, the University of Babylon, college of science and College of science for women, department of chemistry.

6. REFERENCES:

1. Goodenqugh, J. B.; and Loeb, A. L. Physical Review. 1955, 98(2), 391.

2. Fritsch, S.; Sarrias, J.; Rousset, A.; Kulkarni, G. U. Materials Research Bulletin. 1998, 33(8), 1185.
3. Boucher, B.; Buh, R.; Perrin, M. Journal of Physics and Chemistry of Solids.1971, 32(10), 2429.
4. Boucher, B.; Burl, R. ; Perrin, M. Journal of Applied Physics. 1971, 42,1615.
5. Bricker, O. Am. Mineral. 1965, 50,1296.
6. Pike, J.; Hanson, J.; Zhang, L.; and Chan, S. Chem. Mater., 2007,19, 5609.
7. McMurdie, H.; Barbara, F.; Sullivan, M.; Mauer, F., A., Part of the Journal of Research of the National Bureau of Standards, 1950, 45, 35.
8. Zhang, P.; Zhan, Y.; Cai, B.; Hao , C.; Wang, J.; Liu, C.; Meng, Z.; Yin, Z.; and Chen, Q. Nano Res . 2010, 3, 235.
9. Yao, J.; Cheng, Y.; Zhou, M.; Zhao, S.; Lin, S.; Wang, X.; Wu, J.; Lia, S.; and Wei, H. Chem. Sci., 2018, 9, 2927.
10. Shah, H. U.; Wang, F.; Toufiq, A. M.; Khattak, A. M.; Iqbal, A.; Ghazi, Z. A.; Ali, S.; Li, X.; Wang, Z. Int. J. Electrochem. Sci. 2016,11,8155.
11. Cui, X.; Li, Y.; Li, S.; Sun, G.; Ma, J.; Zhang, L.; Li, T.; Ma, R. J. Chem. Sci. 2014, 126(3), 561.
12. Vijayalakshmi, S.; Pauline,S. International Journal of ChemTech Research. 2014, 6(7), 3813.
13. Zhao, J.; Xu, L.; Xie, T.; Xie, C. Chin. J. Geochem. 2015, 34(1), 55.
14. Bousquet-Berthelin, C., Stuerga, D., J. Mater. Sci., 2005,40, 253.
15. Themsirimongko, S.; Promsawan, N.; Saipanya, S. Int. J. Electrochem. Sci., 2016,11, 967.
16. Bikkarolla, S. K.; Yu, F.; Zhou, W.; Joseph, P.; Cumpsond, P.; Papakonstantinou, P. J. Mater. Chem. A. 2014, 1.
17. Silvaa, G. C.; Almeidab, F. S.; Ferreirab, A. M.; Ciminellia, V. S. T. Materials Research. 2012, 1.
18. Li, X.; Yang, L. Advanced Materials Research, 2013, 750-752, 1822.
19. Rahaman, H.; Barman, K.; Jasimuddin, S.; Ghosh, S. K. J. Appl. Phys., 2000, 87, 1318.
20. Deepa, G.; Mahadevan, C. K. IOSR Journal of Applied Physics, 2013, 5, 15.
21. Mohammad, S.H.; Haris, K.; Hassan, M.F.; Hayati Idris, N. European International Journal of Science and Technology, 2014, 3(9), 61.
22. Asif, S. A.; Khan, S. B.; Asir, A. M. Nanoscale Research Letters. 2015, 10, 355.
23. Senthilkumar, P.; Rajeswari,P.; and Dhanuskodi, S. Materials, Devices, and Applications XIV, 2015, 9347, 9347IV-1.
24. Hadjiioannoy, T. P.; Christian, G. D.; Efstathion, C. E.; and Nikolelis, D. P. Problem and Solvent in Analytical Chemistry, Pergamon Press, New York, 1988, 341.
25. Ingle, J. D.; Stanley, R. C., Spectrochemical Analysis, Prentice Halli, New York, 1988, 386.
26. Palache, C., Berman, H.; and Frondel, C.; Dana's system of mineralogy, 7th edition, I, 1944, 712.
27. Hussein, Z. A.; Abbas, S. K.; and Ahmed, L. M. IOP Conference Series: Materials Science and Engineering. 2018, 454, 1.
28. Ahmed, L. M.; Jassim, M. A.; Mohammed, M. Q. and Hamza, D.T. Journal of Global Pharma Technology, 2018,10, 248.
29. Ahmed, L. M. Asian J. Chem., 2018, 30(9), 2134.
30. Kzar, K. O.; Mohammed, Z. F.; Saeed, S. I.; Ahmed, L. M.; Kareem, D. I.; Hadyi, H. and Kadhim, A. J. AIP Conf. Proc., 2019, 2144, 020004-1.
31. Rangel, E. M.; Carvalho, C. De O.; Arsand, D. R. PERIÓDICO TCHÊ QUÍMICA. 2018, 15 (29), 7-81.
32. Mohammed, B. A., and Ahmed, L. M. Journal of Global Pharma Technology. 2018, 10(7), 129.
33. Fakhri, F. H., and Ahmed, L. M., Indones. J. Chem.,2019, 19(4), 936.
34. Vaizoğullar, A.I.; Balci, A.; Uğurlu, M. and Karaoğlu, M. H. AKU J. Sci. Eng. 2016,16, 54.
35. Mahammed, B. A.; and Ahmed, L. M. Journal of Geoscience and Environment Protection. 2017,5, 101.
36. Ahmed, L. M.; Ivanova, I.; Hussein, F. H.; and Bahnemann, D. W. International Journal of Photoenergy. 2014,1.
37. Ghosh, D. C., and Biswas, R. Int. J. Mol. Sci. 2003, 4, 379.
38. Brijnandan, M., Dehiya, S., and Yadav, A. International Journal of Engineering Technology Science and Research. 2017, 4(7), 370.
39. Augustine, C.; and Nnabuchi, M., N. Journal of Non - Oxide Glasses. 2017, 9(3), 85.
40. Ahmed, L. M., Saaed, S. I., and Marhoon, A. A. Indones. J. Chem. 2018, 18(2), 272.
41. Abbas, S. K., Hassan, Z. M., and Ahmed,

L. M. IOP Conf. Series: Journal of Physics: Conf. Series.2019,1294, 1.
42. Ahmed, L. M., Hussen, F. H., and Mahdi, A. A. Asian Journal of Chemistry. 2012, 24(12), 5564.

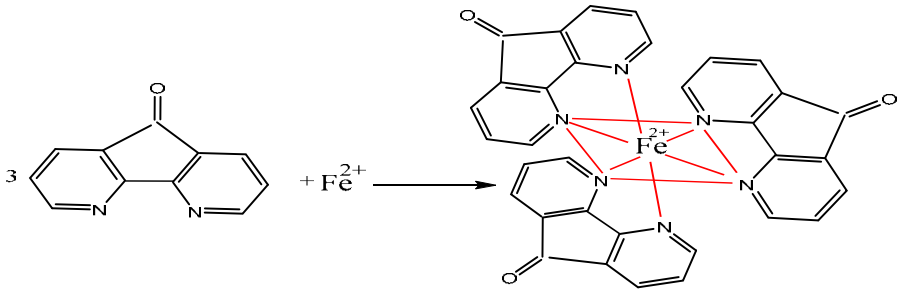

(Eq. 1)

(Eq. 2)

$$k_{instability} = \frac{[Fe^{2+}][L]^3}{[FeL_3]} = \frac{\left[1-\frac{A}{A_{max}}\right]^4}{\left[\frac{A}{A_{max}}\right]} \text{ x } C_{Fe^{2+}} \quad \text{(Eq. 3)}$$

$$= \frac{\left[1-\frac{0.10}{0.172}\right]^4}{\left[\frac{0.10}{0.172}\right]} \text{ x } 2.5 \text{ x } 10^{-3} = 1.320 \text{ x } 10^{-5} \text{ M}$$

$$k_{stability} = \frac{1}{k_{instability}} \quad \text{(Eq.4)}$$

$$= \frac{1}{1.320 \text{ x } 10^{-5}} = 7.575 \text{ x } 10^{4} \text{ M}^{-1}$$

$$Mn(CH_3COO)_2.4H_2O + Na_2CO_3 \rightarrow MnCO_3 + 2\,CH_3COONa \quad \text{(Eq. 5)}$$

$$3MnCO_3 + \frac{1}{2}O_2 + heat \rightarrow MnO.Mn_2O_3 + 3\,CO_2 \quad \text{(Eq. 6)}$$

FeL_3 complex + photocatalyst + UV ⟶ No reaction (Eq. 10)

FeL_3 complex + photocatalyst + H_2O_2 + UV ⟶ Reaction (Eq. 11)

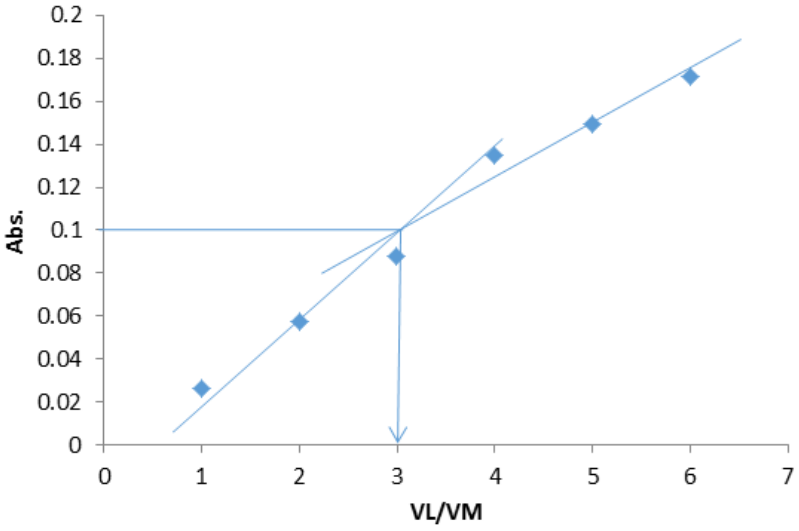

Figure 1. *Mole ratio method for ligand: Fe(II).*

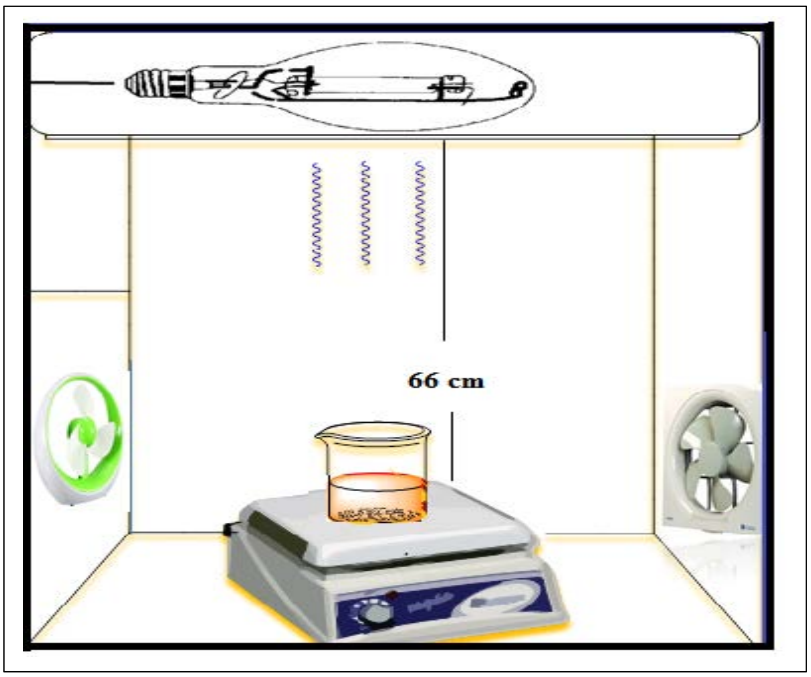

Scheme 1. Schematic diagram of Homemade Photocatalytic Reactor Unit

***Figure 3**. XRD pattern of prepared spinel Mn_3O_4 nanoparticle and his nanocomposites with ZrO_2.*

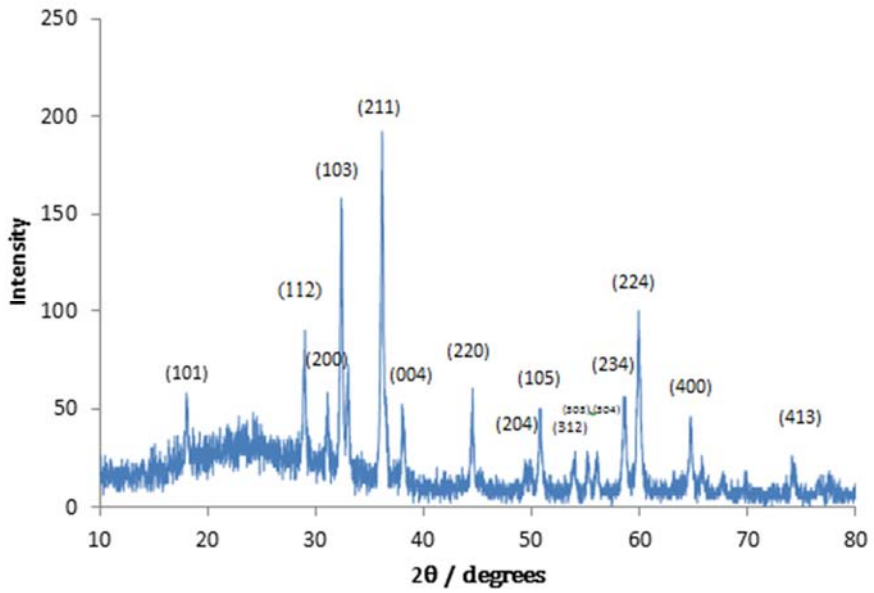

***Figure 2**. XRD pattern of prepared spinel Mn_3O_4 nanoparticle.*

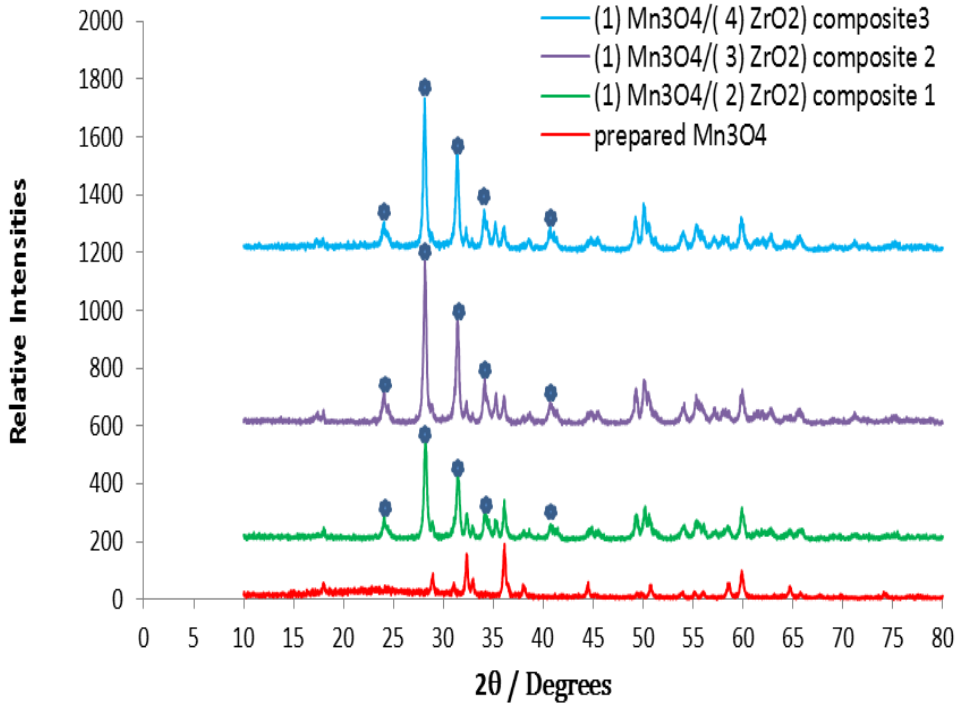

***Figure 3**. XRD pattern of prepared spinel Mn_3O_4 nanoparticle and his nanocomposites with ZrO_2.*

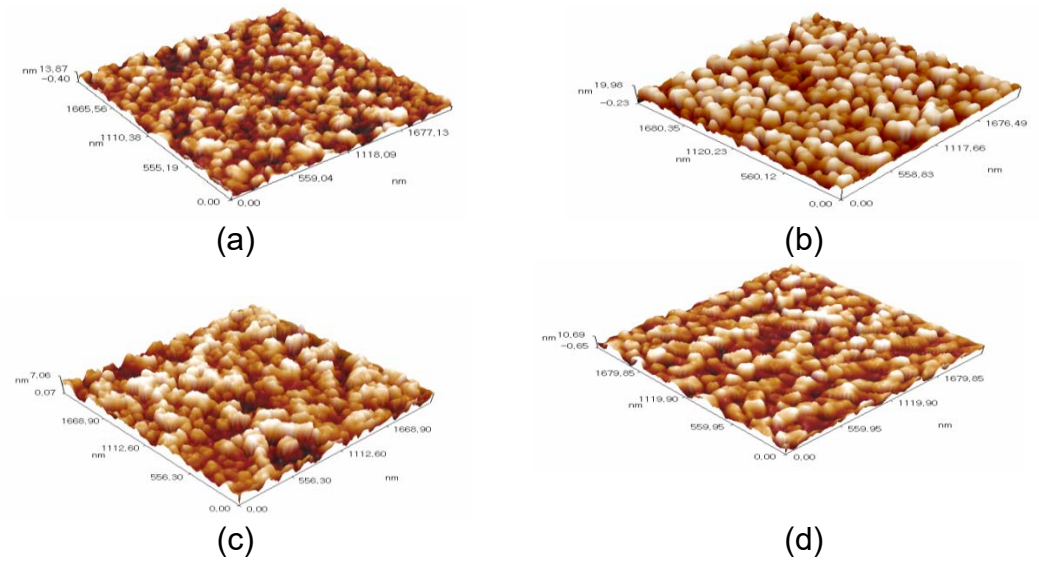

***Figure 4**. AFM Analysis of prepared spinel Mn_3O_4 nanoparticle (a) and his nanocomposites 1, 2 and 3 with ZrO_2 in (b),(c), and (d), respectively.*

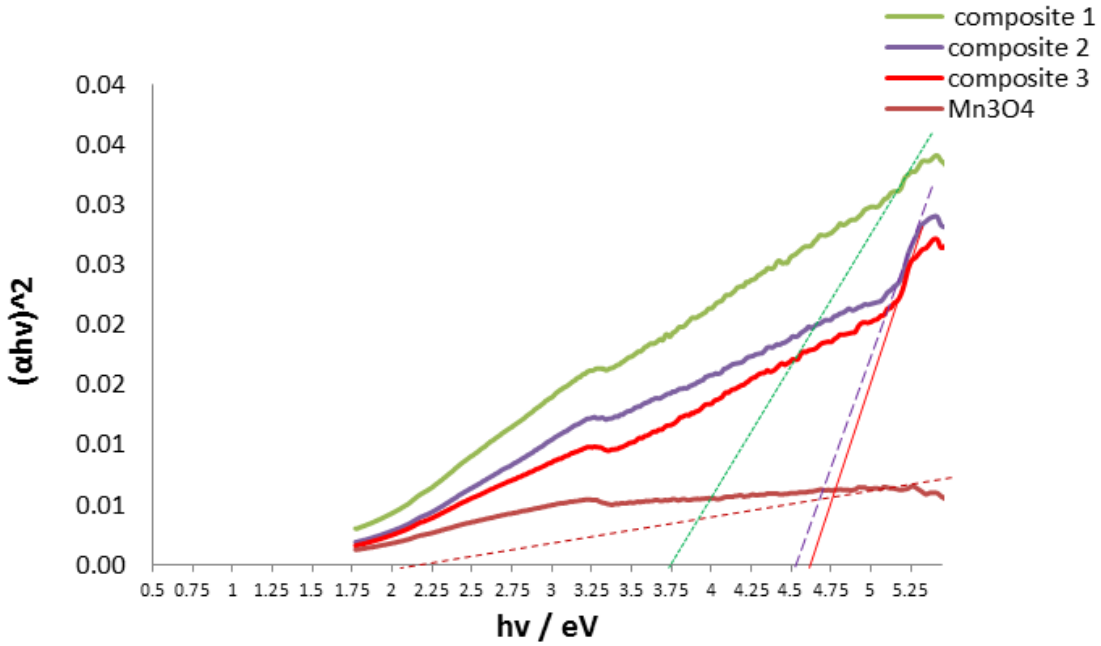

***Figure 5.** The bandgap of prepared spinel Mn_3O_4 nanoparticle and his nanocomposites 1, 2, and 3.*

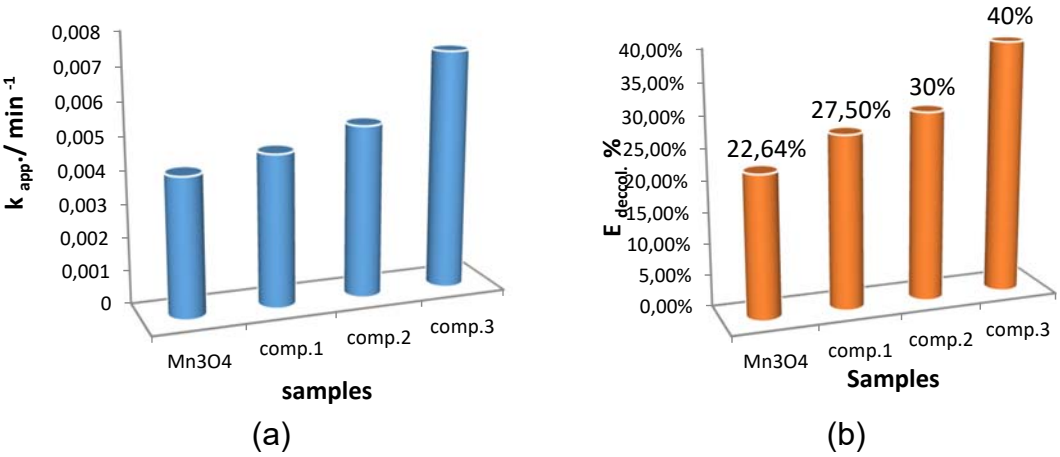

Figure 6. *Photocatalytic decolorization of Fe(II)-(4,5-Diazafluoren-9-one 11) complex by using prepared spine Mn_3O_4 nanoparticle and his nanocomposites 1,2 and 3. (a) Relation between rate constant and samples and (b) $E_{decol.}$% verse samples.*